

MIT Open Access Articles

*On the Kinematics of Solar Mirrors Using
Massively Parallel Binary Actuation*

The MIT Faculty has made this article openly available. **Please share**
how this access benefits you. Your story matters.

Citation: Lee, Seung J., Amy M. Bilton, Steven Dubowsky. "On the Kinematics of Solar Mirrors Using Massively Parallel Binary Actuation." Proceedings of the ASME 2010 International Design Engineering Technical Conferences & Computers and Information in Engineering Conference IDETC/CIE 2010 August 15-18, 2010, Montreal, Quebec, Canada.

As Published: <http://www.asmeconferences.org/idehc2010/>

Publisher: American Society of Mechanical Engineers

Persistent URL: <http://hdl.handle.net/1721.1/60294>

Version: Author's final manuscript: final author's manuscript post peer review, without publisher's formatting or copy editing

Terms of use: Attribution-Noncommercial-Share Alike 3.0 Unported



DETC2010-28875

ON THE KINEMATICS OF SOLAR MIRRORS USING MASSIVELY PARALLEL BINARY ACTUATION

Seung J. Lee

Department of Aeronautics and Astronautics
Massachusetts Institute of Technology
Cambridge, MA 02139
seunglee@mit.edu

Amy M. Bilton

Department of Aeronautics and Astronautics
Massachusetts Institute of Technology
Cambridge, MA 02139
bilton@mit.edu

Steven Dubowsky

Department of Mechanical Engineering
Massachusetts Institute of Technology
Cambridge, MA 02139
dubowsky@mit.edu

ABSTRACT

Precision mirrors are required for effective solar energy collectors. Manufacturing such mirrors and making them robust to disturbances such as thermal gradients is expensive. In this paper, the use of parallel binary actuation to control the shape of mirrors for solar concentrators is explored. The approach embeds binary actuators in a compliant mirror substructure. Actuators are deployed in a specified pattern to correct the mirror shape. The analysis for binary-actuated compliant mirror structures is presented. Analytical models are developed for one-dimensional and two-dimensional compliant structures with embedded binary actuators. These analytical models are validated using finite element analysis and experimental studies. The models and experiments demonstrate the capabilities of binary actuated mirrors. System workspace is explored, the principle of superposition required for their control is demonstrated, as is the mirror ability to correct its figure.

1 INTRODUCTION

Large scale solar concentrators such as parabolic troughs and dishes, such as those seen in Figure 1, are composed of custom precision mirrors. Manufacturing precision mirrors for solar concentrators and making them robust to disturbances such as wind and thermal warping is expensive. Imprecision in mirror shape due to manufacturing limitations and disturbances

degrades the performance of solar concentrator systems [1-3]. Embedding simple, inexpensive binary actuators in the mirror structure to correct the shape can decrease manufacturing costs and improve system performance.



Figure 1: Solar concentrators composed of faceted mirrors [1].

Using embedded actuators to actively control a structure's shape is complex and has been a topic of research [4-7]. Mirrors in large space telescopes like the James Webb use complex continuous actuators to correct the shape of the primary mirror [4, 5]. Researchers have also developed smart structures by embedding continuous actuators and sensors in a structure to control its shape [6, 7]. These solutions have many

drawbacks, including high complexity, low reliability and the need for a large number of actuators and feedback sensors.

Binary actuators can potentially simplify the design of these structures. Binary actuators have two discrete output states, either fully extended or contracted. In the past, conventional elements, such as pneumatic pistons and solenoids, have been used to drive bi-stable mechanisms. Recent studies have shown the potential of using simple, lightweight, low-cost dielectric elastomer actuators (DEA) to activate bi-stable mechanisms [8, 9]. Researchers have studied the use of these binary actuators in serial robotic manipulators [10-14]. A binary manipulator concept developed for space robotics applications is BRAID, shown in Figure 2 [12]. In this approach, a binary manipulator is developed by linking together a series of actuated stages. Each stage has three binary-actuated linkages, resulting in 8 distinct configurations. As the number of stages increases, the capability of the manipulator approaches that of a continuous system.

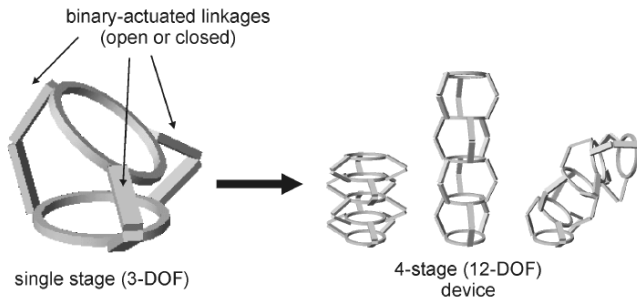


Figure 2: BRAID concept [12].

Many researchers have studied the kinematics of these serial binary robotic systems [12-14]. The workspace for binary robotic manipulators consists of a finite set of points rather than a continuous volume. As such, the inverse kinematics problem of finding an input configuration for the desired end-effector location involves searching through a discrete set of input configurations and finding the one that best matches the desired state. This is not a trivial problem, and simple techniques to evaluate the system workspace are required.

Binary actuators have also been configured in parallel inside a robotic manipulator. Binary dielectric elastomer actuators have been used to develop an MRI compatible manipulator [15]. In this design, binary actuators are configured in a simple parallel planar arrangement to achieve the desired system precision. This parallel configuration results in an over constrained system. These extra constraints are accommodated by adding compliance to the system. This compliance mediates the binary actuations to achieve high precision positioning through “Elastic Averaging” [16].

This paper presents a related approach to correct manufacturing imperfections and shape deformations for solar concentrators. In this approach, binary actuators are embedded in a compliant mirror substructure. Actuators are deployed in a

specified pattern to correct the mirror shape. The precision of the binary actuated system is determined by location and number of actuators. As the number of actuators in a system increases, the precision of the device approaches a conventional continuous system.

The binary actuation approach has many potential advantages. Binary actuators are simple, inexpensive, and lightweight. Also, the binary actuated systems are robust due to their redundancy. Failure of individual binary actuators would result in a graceful degradation of performance. In addition, since the actuator output is discrete, active low-level actuator sensors or feedback control is not necessary and computations for figure control can be performed offline. Also, binary actuators are energy efficient as power is only required to change their states.

This paper presents methods to analyze binary-actuated compliant mirror structures. Analytical models are developed for one-dimensional and two-dimensional compliant structures with embedded binary actuators. These analytical models are validated using finite element analysis and experimental studies. The models and experiments are used to demonstrate the capabilities of binary actuated mirrors by exploring the system workspace, demonstrating the principle of superposition, and evaluating the precision of figure correction.

2 SIMPLE ONE-DIMENSIONAL STRUCTURE

2.1 SYSTEM MODEL

The simplest structure that captures the essence of the parallel binary actuation problem is shown in Figure 3. It is termed here the Binary Beam Model or BBM. In this model, the beam represents the mirror surface and it is supported by binary actuators connected in series with elastic elements. The actuators are placed perpendicular to the beam and are assumed to rigid in the x direction, allowing only one degree of freedom. In addition, the actuators are equally spaced along the beam, are connected to the beam via pin joint and are fixed to ground, preventing any rotations or translations at the base. In this analysis, it is assumed that the actuators are able to produce any required forces to achieve their bi-stable positions. Also, it is assumed that the beam is uniform and that the displacements are small.

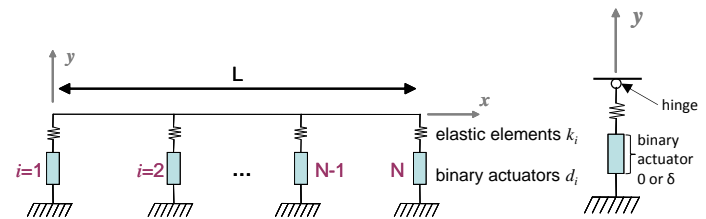


Figure 3: Binary Beam Model (BBM).

2.2 ANALYTICAL DEVELOPMENT

An analytical model of the binary beam structure can be written based on Euler-Bernoulli beam theory. For a beam with uniform cross-section and stiffness, the Euler-Bernoulli beam equation becomes:

$$\frac{\partial^2 y}{\partial x^2} = \frac{M(x)}{EI} \quad (1)$$

where y is the beam deflection, $M(x)$ is the bending moment, E is the Young's modulus of the beam, and I is the beam area moment of inertia. By integrating equation (1) and applying the static equilibrium conditions, the slope and displacement between actuator $i-1$ and actuator i can be found using:

$$y_i'(x) = \frac{1}{EI} \sum_{j=1}^i \left[\left(-\frac{1}{2} k x^2 + k \left(\frac{(j-1)L}{N-1} \right) x \right) y_j \right] + \frac{1}{EI} \left(\sum_{j=1}^i \left[\left(\frac{1}{2} k x^2 - k \left(\frac{(j-1)L}{N-1} \right) x \right) d_j \right] + C_i \right) \quad (2)$$

$$y_i(x) = \frac{1}{EI} \sum_{j=1}^i \left[\left(-\frac{1}{6} k x^3 + \frac{1}{2} k \left(\frac{(j-1)L}{N-1} \right) x^2 \right) y_j \right] + \frac{1}{EI} \left(\sum_{j=1}^i \left[\left(\frac{1}{6} k x^3 - \frac{1}{2} k \left(\frac{(j-1)L}{N-1} \right) x^2 \right) d_j \right] + C_i x + D_i \right) \quad (3)$$

where y_i is the beam deformation at the i^{th} actuator, k is the stiffness of the elastic element, L is the beam length, N is the total number of actuators, and d_i is the displacement of the i^{th} actuator. C_i and D_i are constants of integration. Since the beam is continuous in both displacement and slope at the actuator locations, the constants of integration are given by:

$$C_i = \sum_{j=2}^i \left(-\frac{1}{2} k \left(\frac{(j-1)L}{N-1} \right)^2 y_j + \frac{1}{2} k \left(\frac{(j-1)L}{N-1} \right)^2 d_j \right) + C_1 \quad (4)$$

$$D_i = \sum_{j=2}^i \left(\frac{1}{6} k \left(\frac{(j-1)L}{N-1} \right)^3 y_j - \frac{1}{6} k \left(\frac{(j-1)L}{N-1} \right)^3 d_j \right) + D_1 \quad (5)$$

where D_1 is given by:

$$D_1 = EI y_1 \quad (6)$$

and C_1 is given by:

$$C_1 = \frac{N-1}{L} \left[\left(\frac{1}{6} k \left(\frac{L}{N-1} \right)^3 - EI \right) y_1 + EI y_2 - \frac{1}{6} k \left(\frac{L}{N-1} \right)^3 d_1 \right] \quad (7)$$

Equations (2) through (7) define the analytical solution for the binary beam model. The equations can be manipulated into the matrix form:

$$\mathbf{y} = \mathbf{A} \mathbf{d} \quad (8)$$

where \mathbf{y} is a vector of beam displacements at the actuator locations and \mathbf{d} is a vector of ones and zeros defining which

actuators are extended (1) and which actuators are contracted (0). Equations (2) and (3) can be used to determine the beam deflection and slope at any point. For more details on the analytical model, refer to [17].

The analytical solution assumes that the actuator displacement is small compared to the length of the beam. This assumption will generally be valid for the corrections required of a large mirror system. Using this matrix form the inverse kinematics that determines the desired actuation for a given set of beam displacements can be found using:

$$\mathbf{d} = \mathbf{A}^{-1} \mathbf{y} \quad (9)$$

This equation will give non-discrete values for \mathbf{d} , making this unrealizable for binary systems. Determining the control input \mathbf{d} that gets a correction closest to the desired output shape is not trivial and will require evaluation of different actuator inputs. Simplified analysis techniques will be required to control these binary systems.

When the small displacement assumption holds, superposition can be used to greatly simplify the analysis, design and control of binary actuated structures. In this approach, the deformation of a structure for some general input can be calculated by adding the deformations for each individual actuator separately. For small displacements, the superposition solution should yield fairly accurate results. If superposition holds, the entire structure workspace can be determined through N structure analysis as opposed to 2^N separate calculations. For complicated structures, this can greatly reduce the required computations.

As geometry becomes more complex and the number of actuators increases, obtaining analytical solutions becomes more difficult. For larger and more complicated geometries, Finite Element Analysis can be used to analyze binary actuated structures. A finite element model for the binary beam structure was developed in ADINA. A sample ADINA output for four-actuator system with an input command of $\mathbf{d}=[0 \ 1 \ 0 \ 0]^T$ is shown in Figure 4.

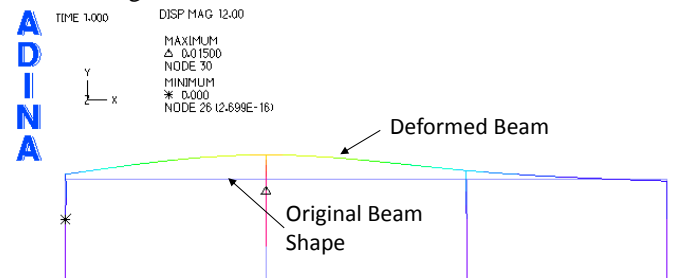


Figure 4: Sample ADINA results.

2.3 ANALYSIS RESULTS

The finite element model was used to validate the analytical model. The structural parameters that were used in the analysis are shown in Table 1. Figure 5 shows a comparison of analytical and FEA results for a 10-actuator BBM. The actuator input for this comparison is given by $\mathbf{d} = [0 \ 0 \ 0 \ 0 \ 1 \ 1 \ 1 \ 1 \ 0 \ 0]^T$

$\begin{bmatrix} 1 & 1 & 1 \end{bmatrix}^T$, a step input to the system. There is good agreement between the two models. The maximum error is on the order of $1\mu\text{m}$.

Table 1: Structural parameters for analytical model validation.

BEAM LENGTH (L)	3 m
BEAM YOUNG'S MODULUS (E)	200 GPa (steel beam)
BEAM CROSS SECTION ($W \times H$)	1 cm X 1 cm
NUMBER OF ACTUATORS (N)	4 and 10
STROKE LENGTH (δ)	1.5 cm
ELASTIC ELEMENT STIFFNESS (k)	2000 N/m

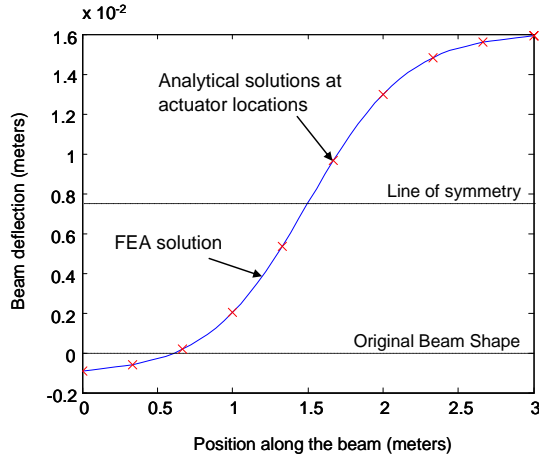


Figure 5: Results for 8-actuator system with step input.

Superposition was tested for the one-dimensional structure using the finite element model. Figure 6 shows the maximum percentage error in the superposition solution versus the actuator displacement for structures with varying number of embedded actuators. In all cases, the maximum error increases exponentially as the actuator displacement increases. The error also increases as the number of actuators embedded in the structure goes up. For all cases, the superposition solution for actuation lengths less than 0.05m has an error that is less than 1%. For small displacements, the superposition solution for the binary beam model gives accurate results.

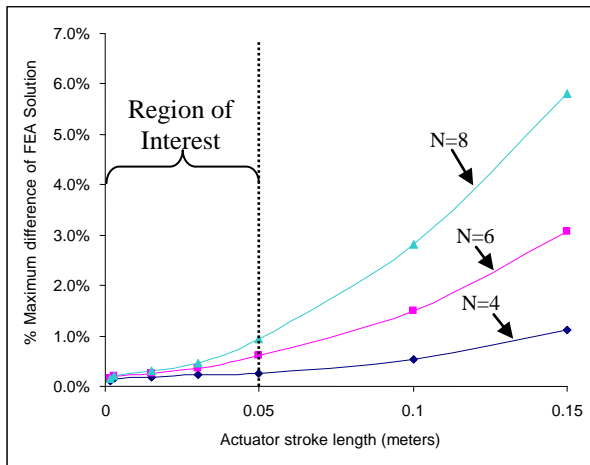


Figure 6: Results of superposition analysis for BBM.

2.4 EXPERIMENTAL VALIDATION

An experimental system was constructed to validate the results from the analytical and FEA models. The experimental setup used is shown Figure 7. In this setup, an 89 cm long stainless steel beam is supported by 10 equally-spaced actuators. To simplify this preliminary experiment, the binary actuation is done manually. The structure compliance is provided by vibration mounts which connect the beam to the manual actuators. Structure displacements are measured along the structure length using a dial indicator. The properties of the experimental system are shown in Table 2.

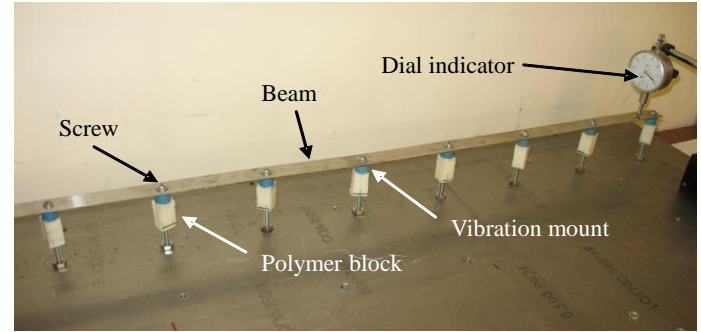


Figure 7: One-dimensional experimental setup.

Table 2: One-dimensional experimental system properties.

BEAM LENGTH (L)	89.9 cm
BEAM YOUNG'S MODULUS (E)	112 GPa
BEAM CROSS SECTION ($W \times H$)	22.6 mm X 0.96 mm
NUMBER OF ACTUATORS (N)	10
STROKE LENGTH (δ)	2.6 mm
VIBRATION MOUNT STIFFNESS (k)	21702 N/m

Sample experimental results for a step input are shown in Figure 8. For a step input, all of the actuators on the right side of the structure are deployed. For this 10-actuator experimental system, the binary input is $\mathbf{d} = [0 \ 0 \ 0 \ 0 \ 0 \ 1 \ 1 \ 1 \ 1 \ 1]^T$. The experimental results are compared to the results from finite element analysis for the same input and good agreement can be seen. The maximum error for any input was less than 10%. These errors can be attributed to uncertainties in the measurements, manual actuation stroke lengths and structural parameters.

In Figure 8, a noticeable “overshoot” can be seen for the step input. This occurs due to the relative stiffness of the beam and the elastic elements. The experimental setup is a “soft system”; the ratio of beam stiffness to elastic element stiffness is low. In a soft system, the beam undergoes large deformations and the majority of the elastic averaging occurs in the beam. In a “hard system”, the ratio of beam stiffness to elastic element stiffness is high and the majority of the elastic averaging occurs in the elastic elements. This effect is shown in Figure 9.

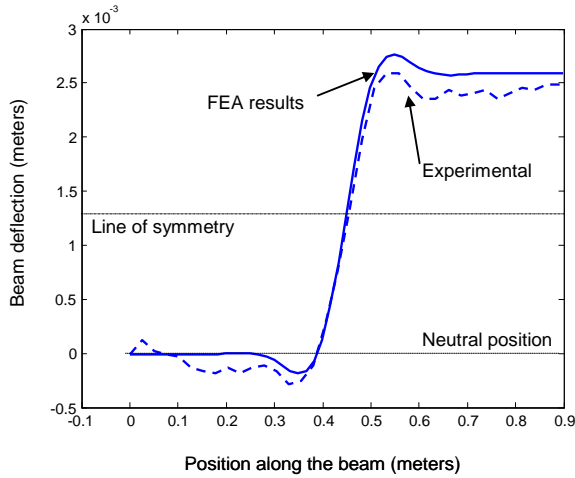


Figure 8: Experimental validation of step input.

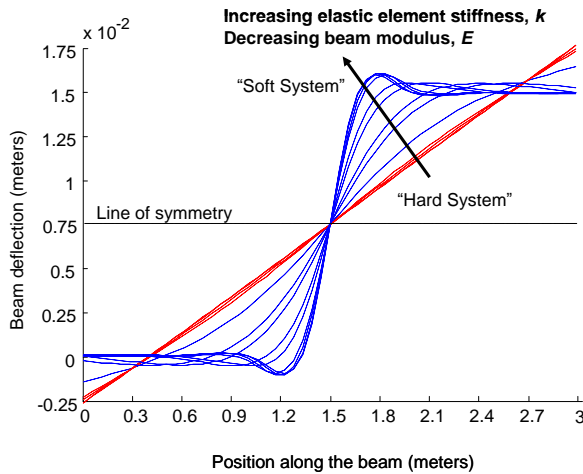


Figure 9: System response to step input for varying system stiffness.

3 TWO-DIMENSIONAL STRUCTURE

The BBM one-dimensional structure provides insight into binary actuated flexible structures. A two-dimensional structure was analyzed to study the capabilities of binary-actuated solar mirrors. A full three-dimensional system was studied experimentally, and is discussed in section 4.

3.1 MODEL

Figure 10 shows the model of the two-dimensional structure. This model is a three-panel mirror structure where the mirrors are joined by flexible beam-like members. The supporting structure contains six embedded actuators which are connected to the mirror panels via pin joints. The properties of the model structure are given in Table 3.

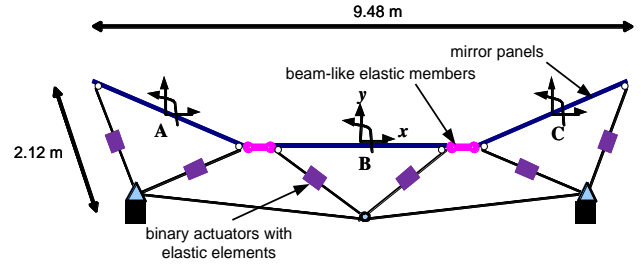


Figure 10: Two-dimensional structure model.

Table 3: One-dimensional experimental system properties.

STRUCTURE LENGTH	9.48 m
FLEXIBLE LINK STIFFNESS (EI)	590 Nm ²
FLEXIBLE LINK LENGTH	0.25 m
NUMBER OF ACTUATORS (N)	6
STROKE LENGTH (δ)	50 mm
ELASTIC ELEMENT STIFFNESS (k)	2000 N/m

3.2 WORKSPACE ANALYSIS AND PERFORMANCE

3.2.1 Single Tier System

An ADINA finite element model was used to analyze the performance of the binary actuated structure shown in Figure 10. The workspace for this system consists of a set of discrete points that indicate the location and orientation of each panel as shown in Figures 11-13. As expected, the set of reachable workspace points is not evenly distributed due to the symmetry of the structure.

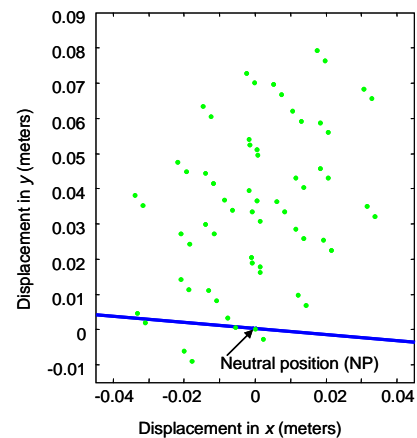


Figure 11: Panel A position workspace.

The clustering of workspace points has been previously noted for binary actuated systems. It has been shown that modifying the structure symmetry spreads the workspace points [15]. Here, this is accomplished by varying the stiffness of the elastic elements connected in series with the actuators, such as shown in Figure 3. Figure 14 shows the workspace for the mirror structure with random elastic elements stiffness. The stiffness are randomly generated using a uniform probability distribution function with bounds of 1000 N/m and 3000 N/m. The workspace for this system is more evenly distributed. It is

more likely that the required shape corrections can be made with this more evenly distributed workspace.

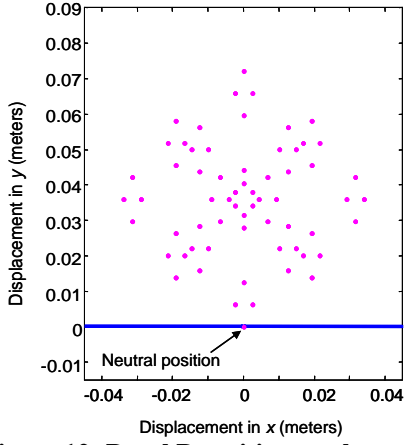


Figure 12: Panel B position workspace.

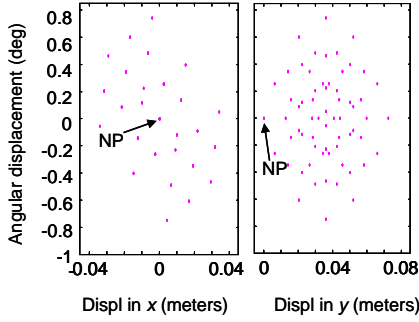


Figure 13: Panel B angular workspace.

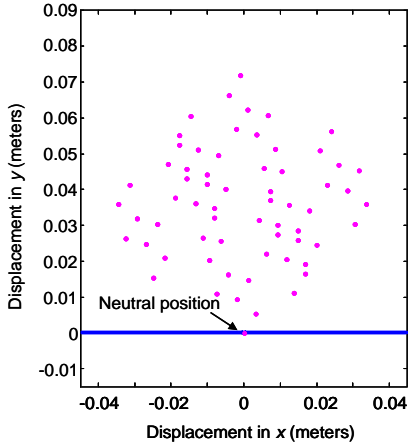


Figure 14: Panel B position workspace with random elastic element stiffness.

The performance of a solar collector is determined by the amount of light collected by the thermal receiver placed in the focal plane of the mirror. Therefore, the performance of the mirrors should be measured based on how the motion of the mirror segments affect the light in the plane. A metric of the system workspace has been formulated to evaluate a binary-actuated mirror system's ability to focus light on the receiver.

For a given system, requirements can be set on the size of the reflected spot (defocus). The smaller the defocus, the better the system will perform. This workspace metric is shown in Figure 16.

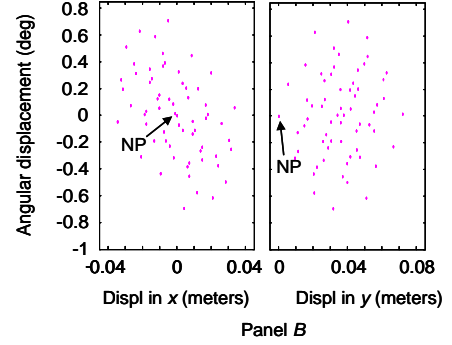


Figure 15: Panel B angular workspace with random elastic element stiffness.

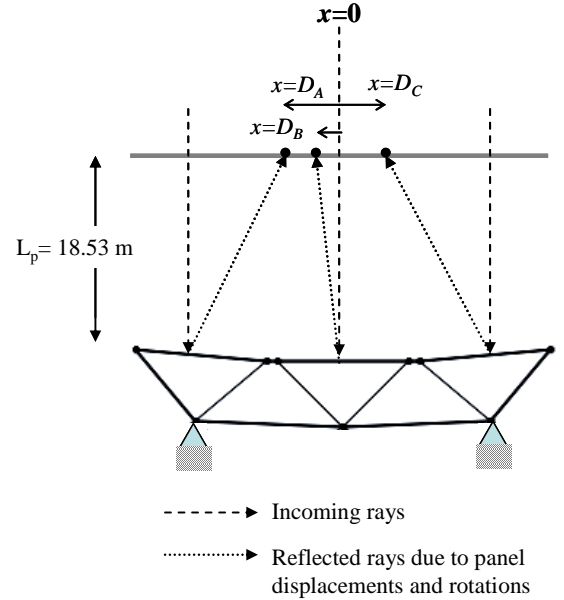


Figure 16: Focal plane workspace for two-dimensional mirror structure.

In this analysis, the workspace is defined by the x-position of the mirror segments focus and the magnitude of the defocus. The position of the focus is defined as the average position of the reflected rays for a given actuator input as given by:

$$f_c(d) = \frac{D_A(d) + D_B(d) + D_C(d)}{3} \quad (10)$$

where $D_A(d)$, $D_B(d)$ and $D_C(d)$ are the positions of the reflected rays in the focal plane for panels A, B, and C respectively. The defocus is defined as the maximum distance between two reflected rays:

$$F_d(d) = \max(D_A(d), D_B(d), D_C(d)) - \min(D_A(d), D_B(d), D_C(d)) \quad (11)$$

Figure 17 shows the focal plane workspace for the one-tier two-dimensional structure with random elastic element stiffness. Despite breaking the structure symmetry by varying the stiffness of the elastic elements, there are still many overlapping solutions in the focal plane. The range of potential focal points for this system is small.

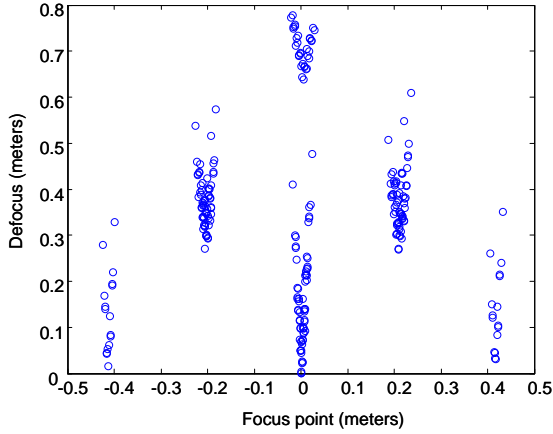


Figure 17: Focal plane workspace for one tier two-dimensional system.

Superposition was tested for the one tier three-dimensional system shown in Figure 10. The resulting maximum percentage errors in panel position and angles for the superposition solutions versus actuator displacement are shown in Figures 18 and 19. In both cases, the errors in the superposition solutions grow exponentially as the actuator stroke length increases. However, for small displacements, superposition gives accurate solutions. For actuator stroke lengths of less than 0.05 m (0.5% of structure size), the superposition solution has errors less than 5%. These values may be large for industrial systems, such as parallel kinematic machines, but are suitable for solar concentrator analysis, design, and control.

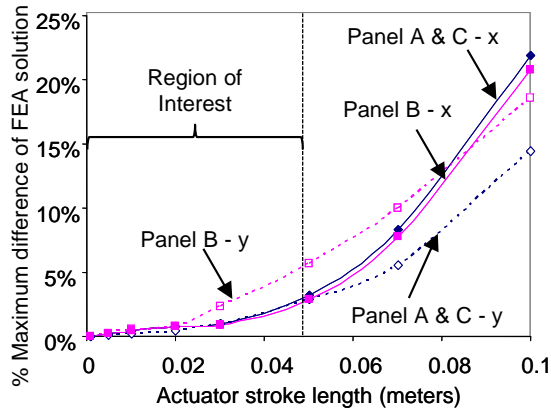


Figure 18: Position superposition results for two-dimensional structure.

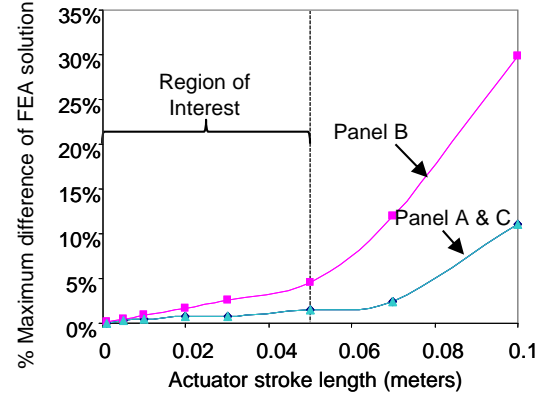


Figure 19: Angular superposition results for two-dimensional structure.

3.2.2 Multi-Tier System

The previous analysis was conducted for a simple one-tier two-dimensional concentrator system. Here, a multiple tier substructure for a solar concentrator system, consisting of a two-tier, two-dimensional system, as shown in Figure 20, is studied. The structure contains 17 binary actuators in series with randomly selected elastic elements. The probability distribution function for the elastic element stiffness and actuator stroke length are identical to the values used in the one-tier system analysis.

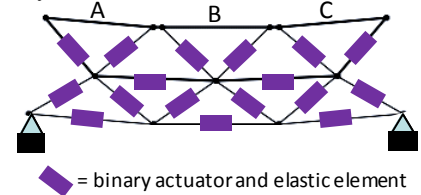


Figure 20: Multilayer two-dimensional system.

The position and angular workspace for the center panel of this two-tier system is shown in Figure 21. The range of motion for the two-tier system is more than double that of the one-tier structure. In addition, with 17 actuators, the workspace is no longer sparse and approaches that of a continuous system.

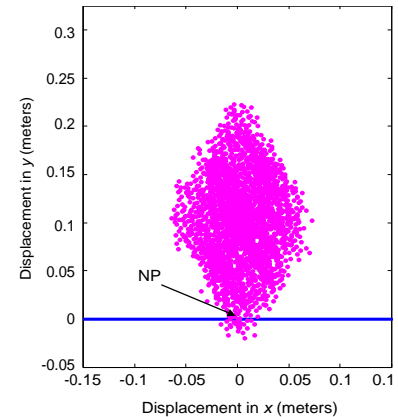


Figure 21: Panel B position workspace for two-tier two-dimensional structure.

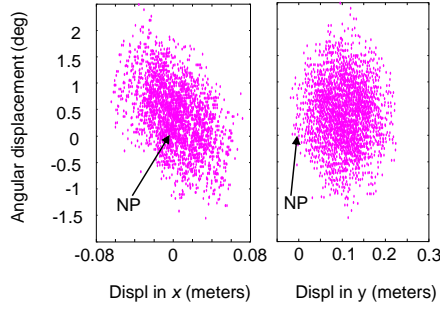


Figure 22: Panel B angular workspace for two-tier two-dimensional structure.

The focal plane workspace for the two-tier system is shown in Figure 23. For this system, the focal plane workspace is also dense. The two-tier system is able to shift the focus of the concentrator in the focal plane. In addition, there are many configurations that have a defocus of less than 10 cm, a reasonable size for a solar concentrator receiver.

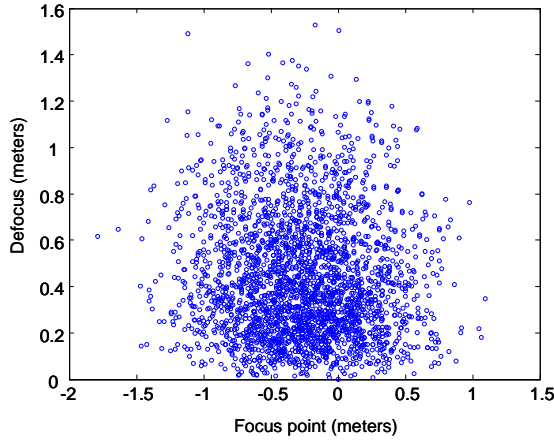


Figure 23: Focal plane workspace for multilayer two-dimensional system.

4 EXPERIMENTAL VALIDATION

A three-dimensional experimental system was designed and built to demonstrate the workspace range and principle of superposition for binary actuated solar concentrator systems. A finite element analysis of the three-dimensional system is beyond the scope of this paper due to space restrictions.

4.1 SYSTEM DESCRIPTION

The three-dimensional experimental system is shown in Figure 24. The binary-actuated mirror consists of 19 hexagonal mirror panels mounted on a compliant plate. The plate is supported by 13 vertical actuators and 30 vertical compliant struts as shown in Figure 25. Due to the force output limitations of current binary actuators, micro-linear actuators manufactured by Firgelli Technologies are used in a binary fashion. The properties of the experimental system are displayed in Table 4.

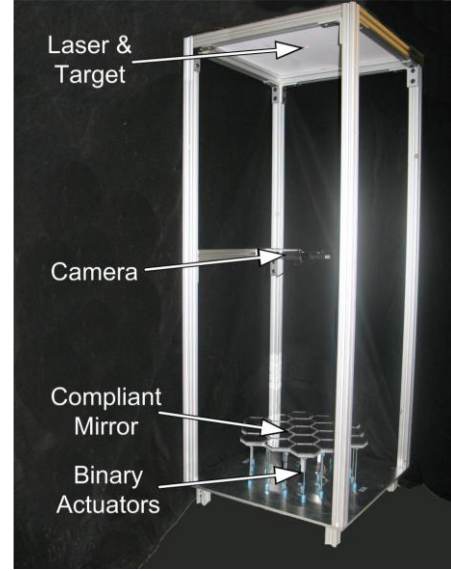


Figure 24: Three-dimensional experimental setup.

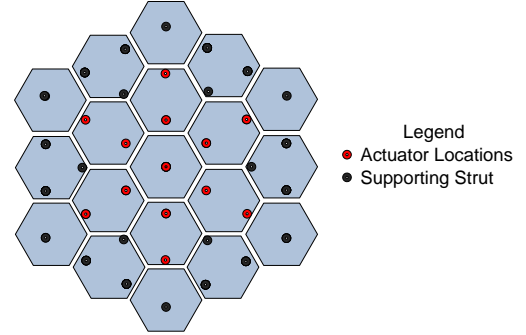


Figure 25: Experimental system actuator layout.

Table 4: Experimental system parameters.

PLATE DIAMETER	480 mm
PLATE YOUNG'S MODULUS (E)	319 MPa
PLATE THICKNESS	12.7 mm
NUMBER OF ACTUATORS (N)	13
NOMINAL STROKE LENGTH (δ)	10.0 mm
VIBRATION MOUNT STIFFNESS (k)	21702 N/m
FOCAL PLANE DISTANCE	1.359 m

In these experiments, the rotational workspace of the center mirror is evaluated. In order to measure the workspace in an automated fashion, a vision-based measurement system was implemented. In this system, a laser beam is reflected off the center mirror onto a focal plane. A CCD camera captures images of the reflected ray in the focal plane. These images are processed to determine the position of the reflected ray and the angular deflection of the center mirror.

4.2 WORKSPACE EVALUATION

The results of the workspace evaluation for uniform elastic element stiffness and actuator displacement of 10mm are shown in Figure 26. With 13 actuators, the system has 8192 (2^{13})

different configurations. As in the two-dimensional analysis, the workspace is symmetric. Also, with uniform elastic element stiffness, the reachable points are clustered, limiting the performance of the binary actuated mirror.

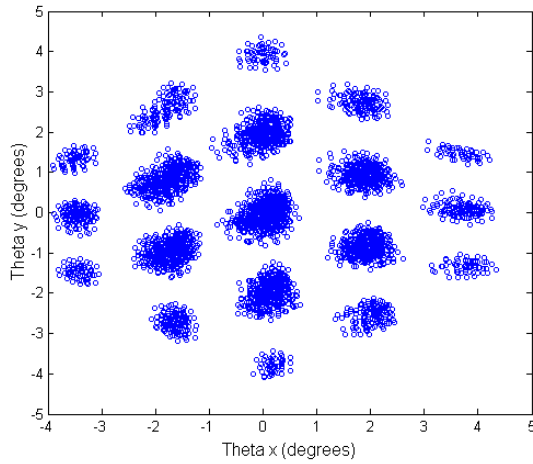


Figure 26: Measured rotational workspace of center mirror of experimental system.

It was shown in the two-dimensional system analysis that the mirror workspace can be more evenly distributed if the structure symmetry is modified by varying the stiffness of the elastic elements. The experimental verification of this effect is shown in Figure 27. In this instance, the range of the workspace has been slightly increased and the workspace clustering has been alleviated. This configuration is suitable for making mirror shape corrections.

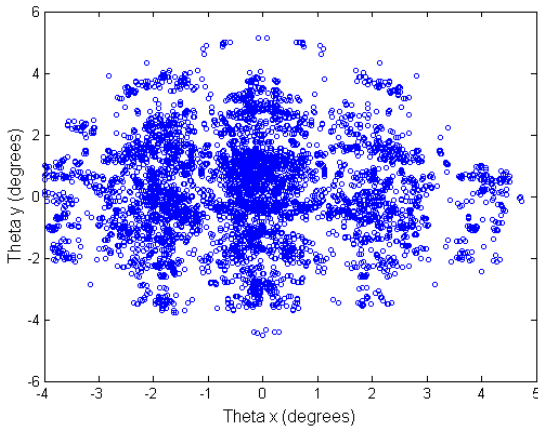


Figure 27: Measured rotational workspace of center mirror with random elastic element stiffness.

4.3 SUPERPOSITION ANALYSIS

Superposition was tested for the three-dimensional experimental system. Figure 28 shows the maximum percentage error in the superposition solution versus the actuator displacement. The trend was found to be similar to previous finite element analysis. The maximum error increases exponentially as the actuator displacement increases.

The errors in the superposition analysis are larger than expected. This occurs because the properties of the experimental system degrade the results of superposition analysis. For example, the linear actuators only mimic binary actuation, and subsequent actuation displacements are not always identical. Also, the mirror-supporting plate consists of a non-uniform honeycomb structure which may exhibit non-linear behavior. Inaccuracy of the measurement system will also degrade results. These aspects will be considered in further analysis, which is beyond the scope of this paper.

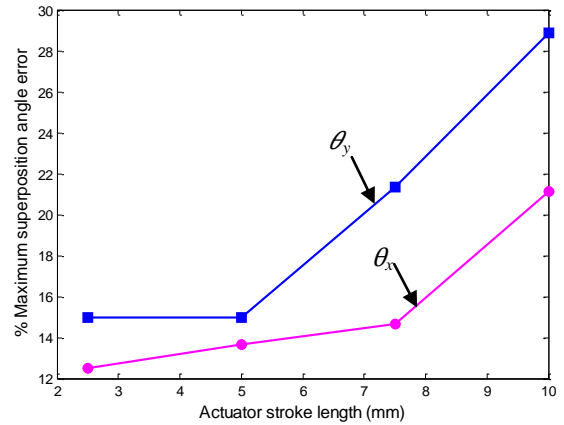


Figure 28: Error in center mirror angle calculation using superposition.

5 SUMMARY & CONCLUSIONS

This paper presents a binary actuation approach to correct shape deformations of solar concentrators consisting of segmented mirror arrays due to manufacturing imprecision and thermal effects. In this approach, binary actuators are embedded in a compliant mirror substructure. Actuators are deployed in a specified pattern to correct the mirror shape.

Analysis techniques for binary-actuated compliant mirror structures are presented. Analytical models are developed for one-dimensional and two-dimensional compliant structures with embedded binary actuators. These analytical models are validated using finite element analysis and experimental studies.

Analytical models and experimental studies are used to demonstrate key features of binary-actuated solar concentrators. Models and experiments are used to show the workspace range of binary structures. For symmetric structures, the workspaces of the mirrors have many clustered points. Models and experiments show that the points in the workspace can be distributed by varying elastic element stiffness and breaking the structure symmetry. Models and experiments are also used to show the range of validity for superposition, a powerful technique that simplifies the analysis, design, and control of binary-actuated structures.

ACKNOWLEDGMENTS

The authors would like to thank Northrop Grumman and the Cyprus Institute for their financial support of this research. The authors would also like to thank Daniel Kettler, Yuanyu Chen, and Lifang Li for their assistance during the development of this work.

REFERENCES

1. Mancini, T., Heller, P., Butler, B., Osborn, B., Schiel, W., Goldberg, V., Buck, R., Diver, R., Andraka, C., and Moreno, J., 2003, "Dish-Stirling Systems: An Overview of Development and Status," *ASME J. of Solar Energy Eng.*, **125**(5), pp. 135-151.
2. Coventry, J. S., 2005, "Performance of a Concentrating Photovoltaic/Thermal Solar Collector," *Solar Energy*, **78**, pp. 211-222.
3. Lüpfert, E., Geyer, M., Schiel, W., Esteban, A., Osuna, R., Zarza, E., and Nava, P., 2001, "Eurotrough Design Issues and Prototype Testing at PSA," *Proc. Of Solar Forum 2001: Solar Energy: The Power to Choose*, Washington, D.C.
4. Gardner, J. P., Mather, J. C., Clampin, M., Doyon, R., Greenhouse, M. A., Hammel, H. B., Hutchings, J. B., Jakobsen, P., Lilly, S. J., Long, K. S., Lunine, J. I., McCaughrean, M. J., Mountain, M., Nella, J., Rieke, G. H., Rieke, M. J., Rix, H., Smith, E. P., Sonneborn, G., Stiavelli, M., Stockman, H. S., Windhorst, R. A., and Wright, G. S., 2006, "The James Webb Space Telescope," *Space Science Reviews*, **123**(4), pp. 485-606.
5. Burge, J. H., Baiocchi, D., Cuerden, B., 2001, "Ultralight Active Mirror Technology at the University of Arizona," *Optomechanical Engineering 2000*, *Proc. Of SPIE*, **4198**.
6. Irschik, H., 2002, "A Review on Static and Dynamic Shape Control of Structures by Piezoelectric Actuation," *Engineering Structures*, **24**, pp. 5-11.
7. Crawley, E. F., 1994, "Intelligent Structures for Aerospace: A Technology Overview and Assessment," *AIAA Journal*, **32**(8), pp. 1689-1699.
8. Wingert, A., Lichter, M. D., and Dubowsky, S., 2006, "On the Design of Large Degree-of-Freedom Digital Mechatronic Devices Based on Bistable Dielectric Elastomer Actuators," *IEEE/ASME Transactions on Mechatronics*, **11**(4), pp. 448-456.
9. Plante, J.S., 2006, "Dielectric Elastomer Actuators for Binary Robotics and Mechatronics," Ph.D Thesis, Massachusetts Institute of Technology, Cambridge, MA.
10. Chirikjian, G. S., 1994, "A binary paradigm for robotic manipulators," *Proc. IEEE Int. Conf. Robotics and Automation*, San Diego, CA, pp. 3063-3069.
11. Lichter, M. D., Sujan, V. A., Dubowsky, S., 2002, "Computational Issues in the Planning and Kinematics of Binary Robots," *Proc. of IEEE Int. Conf. on Robotics and Automation*, Washington, D.C., pp. 341-346.
12. Wingert, A., Lichter, M.D., and Dubowsky, S., 2002, "On the Kinematics of Parallel Mechanisms with Bi-Stable Polymer Actuators," *The 8th International Symposium on Advances in Robot Kinematics*.
13. Ebert-Uphoff, I., and Chirikjian, G. S., 1996, "Inverse Kinematics of Discretely Actuated Hyper-Redundant Manipulators Using Workspace Densities," *Proc. of IEEE Int. Conf. on Robotics and Automation*, Minneapolis, MN, pp. 139-145.
14. Mukherjee, S., and Murlidhar, S., 2001, "Massively Parallel Binary Manipulators," *Transactions of the ASME*, **123**, pp. 68-72.
15. Devita, L., Plante, J.S., and Dubowsky, S., 2007, "The Design of High Precision Parallel Mechanisms using Binary Actuation and Elastic Averaging: With Application to MRI Cancer Treatment," *Proceedings of the 2007 IFToMM World Congress on Machines and Mechanisms*, Besanson, France.
16. Slocum, A., 1992, *Precision Machine Design*, Prentice Hall, Englewood Cliffs, New Jersey.
17. Lee, S.J., 2010, "Planar Feasibility Study for Primary Mirror Control of Large Imaging Space Systems Using Binary Actuators," M.S. Thesis, Massachusetts Institute of Technology, Cambridge, MA.